

# Identification of Candidate Genes Associated with Steroid-Induced Osteonecrosis of The Femoral Head by Bioinformatics Based on GEO Database

**Shile Cheng**

Wuhan University Renmin Hospital <https://orcid.org/0000-0001-8692-3807>

**Zhigang Nie**

Renmin Hospital of Wuhan University: Wuhan University Renmin Hospital

**Hao Peng** (✉ [penghaowhu@126.com](mailto:penghaowhu@126.com))

Renmin Hospital of Wuhan University: Wuhan University Renmin Hospital

---

## Research article

**Keywords:** Osteonecrosis, Genes, Bioinformatics, MicroRNAs

**Posted Date:** October 22nd, 2020

**DOI:** <https://doi.org/10.21203/rs.3.rs-94892/v1>

**License:**  This work is licensed under a Creative Commons Attribution 4.0 International License.

[Read Full License](#)

---

# Abstract

**BACKGROUND** Steroid-induced osteonecrosis of the femoral head (SONFH) is a progressive bone disorder and its characterized by femoral head collapse and hip joint dysfunction and the biomarkers of SONFH remain unclear. The purposes of this study are to identify the significant biological function and pathway involved in SONFH, and further to search the underlying mechanism of this pathway in SONFH.

**METHODS** The GSE123568 dataset obtained from the Gene Expression Omnibus (GEO) database and normalized using Robust Multiarray Averaging (RMA) methods. And the Gene set enrichment analysis (GSEA), Ingenuity pathway analysis (IPA), VarElect online tool, MalaCards database, miRWalk online tool, DIANA too, and Cytoscape were integrated for bioinformatics analyses.

**RESULTS** 6 biological processes and 4 KEGG pathways were enriched by GSEA, and 68 candidate genes were involved in these pathways. Besides, the canonical pathway and molecule function analysis by IPA, the results revealed that 10 canonical pathways and 12 candidate genes were identified, and 20 modules and 101 candidate genes were enriched by molecule function analysis. The above candidate genes were combined and filtered using the VarElect online tool. The filtered candidate genes were overlapped with another cluster of candidate genes from the MalaCards database to identify hub genes ACP5, TNF, MMP8. Based on the hub genes, the miRNAs were screened and overlapped to predict the lncRNAs. Total 7 miRNAs of ACP5, TNF, MMP8 were targeted 956 candidate lncRNAs.

**CONCLUSIONS** In summary, this study identified the hub candidate genes and pathways associated with SONFH progress, and constructed the ceRNA network based on the hub candidate genes. Our findings might provide the potential biomarkers of SONFH diagnosis and treatment.

## Introduction

Osteonecrosis, also known as aseptic necrosis, avascular necrosis, atraumatic necrosis, and ischemic necrosis, is a pathologic process that has been associated with numerous conditions and therapeutic interventions. According to numerous reports, there are approximately 25000 new patients who are diagnosed with osteonecrosis every year, accounting for about 10% of the 250000 total hip arthroplasties done annually in the United States<sup>1,2</sup>. Osteonecrosis usually occurs in the anterolateral femoral head, although it may also affect the femoral condyles, humeral heads, proximal tibia, vertebrae, and small bones of the hand and foot<sup>3</sup>. The previous studies have demonstrated that steroid is an established risk factor of osteonecrosis of the femoral head (ONFH)<sup>4-6</sup>. Moreover, numerous researches have proved that the mechanism of steroid-induced osteonecrosis of the femoral head (SONFH) including oxidative stress<sup>7</sup>, osteoclasts activation<sup>8</sup>, bone formation and resorption<sup>9</sup>, et al. SONFH most have been diagnosed by magnetic resonance imaging (MRI)<sup>5</sup>. However, the reliable biomarkers of SONFH remained unknown.

Long non-coding RNAs (lncRNAs) are a group non-coding RNAs with length more than 200 nucleotides functioning as a competing endogenous RNAs (ceRNAs), which regulate target genes by competing for

shares microRNAs<sup>10,11</sup>. It has been reported that lncRNAs act as the important regulators in SONFH through functioning as ceRNAs of miRNAs and target genes<sup>12</sup>. For example, lncRNA RP11-154D6 promotes osteogenic differentiation and inhibits adipogenic differentiation in bone marrow mesenchymal stem cells (BMSCs) to contribute SONFH progress<sup>13</sup>. lncRNA RP1-193H18.2, MALAT1, and HOTAIR were proved association with abnormal osteogenic and adipogenic differentiation of BMSCs in the patients with SONFH<sup>14</sup>. However, the functions and mechanisms of lncRNA have been entirely unknown in SONFH.

Taken together, we used bioinformatic methods to identify the differentially expressed genes of SONFH, and to enrich the SONFH related pathways. Based on the candidate genes to construct lncRNA-miRNA-mRNA network in SONFH. Our findings revealed the candidate genes and key pathways of SONFH and proved the potential biomarkers of SONFH.

## **Materials And Methods**

### **Data acquiring and processing**

The mRNA expression profiles of SONFH (GSE123568) were acquired from GEO database. The GSE123568 dataset was performed using Affymetrix EG1.0 array, including the peripheral serum of 30 SONFH patients and 10 non-SONFH patients (following steroid administration). RMA was used for the background correction of raw mRNA expression data, and then processed signals were log<sub>2</sub> transform and normalize through quantile normalization. Furthermore, the median-polish probe sets were summarized using affy R package. The quality was assessed by samples clustering based on the distance between different samples in average linkage.

### **Gene set enrichment analysis (GSEA)**

The SONFH samples were divided into two groups according to the mRNA expression levels of GSE123568 dataset by the GSEA software. c5.all.v7.1.symbols.gm and c2.cp.kegg.v7.1.symbols.gm from molecular signature database (MSigDB) version 6.2 were selected as the reference gene set. The gene sets > 500 and gene sets < 15 were used as the excluded criteria. The significant gene sets were identified according to a threshold FDR < 0.25 and P-value < 0.05.

### **Ingenuity pathway analysis (IPA)**

The common DEGs of GSE123568 were uploaded into Qiagen's IPA system for core analysis according to the gene sets of the ingenuity knowledge base. IPA was used to screen canonical pathways associated with common DEGs, and explore the association between diseases and gene function. P-value < 0.05 and | Z-score | > 2 used as the threshold.

### **Correlation between candidate genes and SONFH analysis**

VarElect is an online tool that entails specifying a gene symbol list imported from an experimental data file (s), together with disease phenotype and symptom terms related to the studied disorder<sup>15</sup>. The candidate genes which enriched by GSEA and IPA were firstly integrated, then uploaded the candidate genes into VarElect online tool (<http://ve.genecards.org>) to rank genes, and point out the candidate genes likely to be related to SONFH. Besides, the human disease database MalaCards (<http://www.malacards.org/>) was used to obtain genes that correlated to SONFH. Moreover, Venn diagrams were applied to calculate the intersections of SONFH related genes mentioned above.

### **lncRNAs-miRNAs-mRNA (ceRNAs) network constructing**

miRWalk (<http://mirwalk.umm.uni-heidelberg.de/>) was used to predict the interaction between miRNA and mRNA, and DIANA-LncBASE Predicted v2 ([http://carolina.imis.athena-innovation.gr/diana\\_tools/web/index.php?r=Incbasev2/index-predicted](http://carolina.imis.athena-innovation.gr/diana_tools/web/index.php?r=Incbasev2/index-predicted)) was used to predicate the interaction between miRNA and lncRNA. The DIANA tool supported two prediction models including based on experimental evidence and software prediction. And the ceRNAs networks were visualized by Cytoscape 3.6.1 software.

## **Results**

### **DEGs identification and pathway enrichment by GSEA**

GSEA was used to enrich the pathways of these genes. The enriched gene sets with a threshold FDR < 0.25 and P-value < 0.05. The results of GSEA revealed that the significantly enriched functions including programmed necrotic cell death (1A, supplementary figure 1A), intracellular lipid transport (1B, supplementary figure 1B), necrotic cell death (1C, supplementary figure 1C), lymph vessel morphogenesis (1D, supplementary figure 1D), hydrogen peroxide catabolic process (1E, supplementary figure 1E), lymph vessel development (1F, supplementary figure 1F). And the pathways enriched in Leishmania infection (1G, supplementary figure 1G), glycosaminoglycan biosynthesis chondroitin sulfate (1H, supplementary figure 1H), and T cell receptor signaling pathway (1I, supplementary figure 1I). The 68 genes involved in these pathways were listed in table1, these genes acted as the candidate genes of SONFH.

### **Canonical pathway and molecule function analysis by IPA**

To further identify the candidate genes associated with SONFH, the IPA was used for core analysis with a threshold |Z-score| > 2 and P-value < 0.05. The canonical pathway analysis revealed that interferon signaling, production of nitric oxide and reactive oxygen species in macrophages, Fcγ receptor-mediated phagocytosis in macrophages and monocytes, TREM1 signaling, iNOS signaling, Gai signaling, neuroinflammation signaling pathway, Tec kinase signaling, and Dendritic cell maturation were activated (figure 2A, table 2), and sirtuin signaling pathway was suppressed (figure 2A, table 2). Production of nitric oxide and reactive oxygen species in macrophages illustrated the highest score (z score = 3.464), and total 12 genes ARG2, IFNGR1, IFNGR2, IRF8, LYZ, NCF1, NCF2, NCF4, RHOQ, SERPINA1, TLR2, TYK2 were involved in this pathway (figure 2A, table 2). Besides, the molecule function analysis indicated that the

differentially expressed genes were enriched in different pathways in SONFH (figure 2B), and the enriched genes were involved in 48 functional modules with a threshold  $|z\text{-score}| > 2$  and  $P\text{-value} < 0.05$ , 20 modules were significantly associated with SONFH (figure 2C, table 3). The function among these modules involved in microvascular injury and intravascular coagulation, oxidative stress, immuno-inflammation, and bone marrow cell activity. Among them, microvascular injury and intravascular coagulation included cell-to-cell signaling and interaction, cellular movement, cardiovascular system development and function, cell-to-cell signaling and interaction, cell morphology. Oxidative stress included free radical scavenging, cardiovascular system development and function, cell-to-cell signaling and interaction, free radical scavenging, molecular transport. Immuno-inflammation included inflammatory response, cell death and survival, cardiovascular system development and function, cell-to-cell signaling and interaction, and cell-mediated immune response. bone marrow cell activity included cellular movement (table 3). And the 101 candidate genes involved in 20 function modules, including chemokine receptors, and immune-related genes, etc. Such as CCR1, CCR2, IGHG3, IGKV1-39 (supplementary table 1).

### **Identification of candidate genes of SONFH**

In order to identify the hub genes, the candidate genes were combined and ranked. Then we identified the most likely genes related to SONFH by VarElect online tool. We found that TNF with the highest correlation score, and TNFSF10, FAS, TNFSF13B, FASLG exhibited higher correlation scores than other candidate genes (Table 4). Moreover, the 32 candidate genes related to SONFH were obtained from the MalaCards database (Table 5). Furthermore, the intersections of SONFH related hub genes were identified by Venn diagrams including ACP5, TNF, MMP8 (figure 3).

### **Construction of ceRNA network of hub genes**

To further investigate the mechanisms of ACP5, TNF, MMP8, the ceRNAs networks of these genes were constructed. The results showed that 372 miRNAs interacted with ACP5, 795 miRNAs interacted with TNF, and 4 miRNAs interacted with MMP8. The intersections of three genes included hsa-miR-7845-5p, hsa-miR-6772-3p, hsa-miR-5010-3p, hsa-miR-4653-5p, hsa-miR-1587 (figure 4A, table 7 and 8). The miRNAs were supported with experimental evidence used as the candidate gene of ceRNAs, including hsa-miR-26b-5p (targeted with MMP8), and hsa-miR-19a-3p, hsa-miR-452-5p, hsa-miR-187-3p, hsa-miR-130a-3p, and hsa-miR-143-3p (targeted with TNF) (table 6). Taken together, the lncRNAs targeted with 11 candidate miRNAs were predicted. And we found that 7 of 11 candidate miRNAs targeted 956 candidate lncRNAs (figure 4B, table 7).

## **Discussion**

SONFH is a progressive bone disorder caused by excessively administrating glucocorticoids and resulted in vascular damage, mechanism stress damage, intraosseous pressure increasing, adipocyte dysfunction, apoptosis, and coagulation dysfunction<sup>5</sup>. In our study, we first identified the biological

function of SONFH, which includes programmed necrotic cell death, intracellular lipid transport, necrotic cell death, lymph vessel morphogenesis, hydrogen peroxide catabolic process, and lymph vessel development. It has been reported that the final step in osteonecrosis is vascular insufficiency to the femoral head, resulting in apoptosis and necrosis<sup>16</sup>. Several recent studies have reported that apoptosis relates to the pathogenesis of osteonecrosis of the femoral head<sup>17,18</sup>. Besides, previous studies have shown that steroid treatment implied the intra-osteoblastic lipid droplets pathology and corresponded to low bone mass with increased bone marrow adiposity<sup>19,20</sup>. Around lymph vessel morphogenesis and development, several studies have indicated that different stem and progenitor cells reside in distinct cellular niches in bone marrow, such as hematopoietic stem cells occupy a perivascular niche and early lymphoid progenitors occupy an endosteal niche<sup>21</sup>.

Besides, we screened significant pathways related to SONFH including leishmania infection, glycosaminoglycan biosynthesis chondroitin sulfate, and T cell receptor signaling pathway. Several studies proved that mice infected with *Leishmania* showed osteonecrosis. In addition, the histopathological analysis demonstrated that mononuclear cells infiltrated in plasma cells richly as well as parasitism of intra-medullary and extra-medullary macrophages intensely, also with bone necrosis areas and discrete cartilaginous tissue involvement<sup>22,23</sup>. Okazaki previously reports that the toll-like receptor (TLR) 4 signaling pathway, which induces inflammatory status, contributes to the pathogenesis of non-traumatic ONFH in rats<sup>24-26</sup>. In Okazaki's another study, it has shown that corticosteroid treatment after the administration of TLR7 or TLR9 ligands causes ONFH in rats, whereas corticosteroids alone failed to induce ONFH in healthy animals. In addition, IRF7 and NF- $\kappa$ B are activated in the liver induced by corticosteroid treatment to trigger the development of ONFH<sup>27</sup>. Taken together, normalization of inflammatory status when treating underlying inflammatory diseases may potentially prevent ONFH in the future.

In addition, Gessner's study has illustrated that the differential expressed IL-9 between the susceptible and resistant mice which infected with *Leishmania*<sup>28</sup>. Moreover, Geng's study also reveals that the production of IL-9 may trigger the cartilage degeneration and destruction in ONFH patients. IL-9 promotes cartilage degeneration, and the effect of IL-9 on cartilage is alleviated by blocking JAK-STAT signaling pathway in a human primary chondrocyte culture model<sup>29</sup>. Furthermore, Chen's study has demonstrated IL-21 promotes cartilage degradation by activating cartilage inflammation through JAK-STAT signaling pathway in ONFH patients<sup>30</sup>. The studies above indicated that immune-related genes act as the critical role in ONFH progression through modulating the cartilage degeneration and destruction.

Furthermore, the IPA was used to further investigate the canonical pathway and molecule function of SONFH. The results revealed that 9 pathways were activated, which includes interferon signaling, production of nitric oxide and reactive oxygen species in macrophages, iNOS signaling, Fc $\gamma$  receptor-mediated phagocytosis in macrophages and monocytes, TREM1 signaling, Gai signaling, neuroinflammation signaling pathway, Tec kinase signaling, and Dendritic cell maturation. In contrast, Sirtuin signaling pathway was suppressed. Besides, the molecule function analysis showed that

oxidative stress, microvascular injury and intravascular coagulation, immune inflammation, and myeloid cells movement were significantly involved in SONFH. Here, we found the production of nitric oxide and reactive oxygen species in macrophages showed the strongest correlation with SONFH based on the highest score. Macrophages play the proinflammatory promoter in necrotic bone, Naga Suresh Adapala et al have reported that the numbers of proinflammatory M1 macrophages are increased in the repair bone tissue, which reveals high expression of proinflammatory cytokines IL-1 $\beta$ , TNF- $\alpha$ , and IL-6 and the pattern recognition receptor TLR4<sup>31</sup>. Another study has proved that TNF- $\alpha$ -mediated alteration of M1/M2 macrophage polarization plays a vital role in the pathogenesis of steroid-induced osteonecrosis, with a dominant position that M1 macrophages in early stage and M2 macrophages in the late stage of osteonecrosis<sup>32</sup>. In our result, production of nitric oxide and reactive oxygen species in macrophages was activated. Generally, macrophages maintain organism homeostasis by receptor-mediated recognition and phagocytic uptake of pathogenic damaged or apoptotic host cells. The necrosis bone tissues are degraded by phagocytosis, which activated by proteolytic enzymes and oxidative burst through the formation of reactive oxygen species (ROS) and nitric oxide (NO). The reaction of superoxide with NO results in the formation of peroxynitrite, which interacts with lipids, DNA, and proteins via direct oxidative reactions or indirect radical-mediated mechanisms<sup>33</sup>. All the studies suggest that oxidative stress significantly associates with necrosis bone may inducing macrophages polarization. In the present study, the oxidative stress related pathways were strongly related to the SONFH, and total 12 genes, such as ARG2, IFNGR1, which were associated with the production of nitric oxide and reactive oxygen species in macrophages pathway. Our finding consists of previous studies. ARG2 plays a vital role in nitric oxide and polyamine metabolism through repressing nitric oxide synthesis and inhibiting inflammatory genes levels in macrophages to interrupt M1 macrophage phagocytosis activity<sup>34,35</sup>.

Based on the above research, the SONFH related candidate genes were filtered by VarElect online tool and then overlapped with the candidate genes from MalaCards database. ACP5, TNF, MMP8 were identified as the hub genes of SONFH.

Tartrate-resistant acid phosphatase 5 (ACP5), a metalloprotein enzyme that belongs to the acid phosphatase family and is known to be expressed by osteoclasts. Furthermore, it has been demonstrated that ACP5 acts as a classic marker for bone resorption and osteoclast differentiation<sup>36</sup>. In Yin's study, ACP5 has increased in human ONFH tissues, and high expression of miR-410 and low expression of Wnt-11 inhibit ACP5 and MMP9 expression in ONFH rats<sup>37</sup>. Fang's study has shown the effects of TNF $\alpha$  on proliferation, angiogenesis, and osteogenesis, and osteogenesis of rat bone mesenchymal stem cells (rMSCs)<sup>38</sup>. TNF- $\alpha$  plays as a mediator of bone destruction by stimulating osteoclastogenesis<sup>39-41</sup>.

Several studies have indicated that MMPs degrades and modifies the components of extracellular matrix and basement membrane and push forward an immense influence on cancer invasion and metastasis<sup>37,42-46</sup>. Previous studies have demonstrated that SNPs in the MMP8 and MMP9 genes associates with risk of osteonecrosis of the femoral head in the Chinese Han population<sup>43,45-47</sup>. Jiang's study has shown a remarkable association between rs11225394 in MMP-8 gene and an increased risk of

ONFH and a significant association between MMP-8 rs2012390 and the decreased risk of ONFH<sup>44</sup>. In Chen's study, MMP-8 rs11225394 and MMP-8 rs2012390 are risky and protective factors of alcohol-induced ONFH<sup>46</sup>. Du et al have speculated that polymorphisms of MMP-8 might have an effect on the inflammation or circulatory impairment of the femoral head<sup>43</sup>.

To further study the function and mechanism of hub genes in SONFH, the 372 miRNAs of ACP5, 795 miRNAs of TNF, 4 miRNAs of MMP8 were screened. And hsa-miR-7845-5p, hsa-miR-6772-3p, hsa-miR-5010-3p, hsa-miR-4653-5p, hsa-miR-1587 were intersected in ACP5, TNF, MMP8. And the lncRNAs were predicted by combination of miRNAs and miRNAs. Then, 7 miRNAs, and ACP5, TNF, MMP8 and lncRNAs.

## Conclusions

In summary, this study identified the hub candidate genes and pathways associated with SONFH progress, and constructed the ceRNA network based on the hub candidate genes. Our findings might provide the potential biomarkers of SONFH.

## Abbreviations

NSFC: National Natural Science Foundation of China

SONFH: Steroid-induced osteonecrosis of the femoral head

GEO: Gene Expression Omnibus

RMA: Robust Multiarray Averaging

GSEA: Gene set enrichment analysis

IPA: Ingenuity pathway analysis

ONFH: Osteonecrosis of the femoral head

MRI: Magnetic resonance imaging

lncRNAs: Long non-coding RNAs

ceRNAs: Competing endogenous RNAs

BMSCs: Bone marrow mesenchymal stem cells

MSigDB: Molecular signature database

ROS: Reactive oxygen species

NO: Nitric oxide

ACP5: Tartrate-resistant acid phosphatase 5

rMSCs: Rat bone mesenchymal stem cells

## Declarations

**Ethics approval and consent to participate:** Not applicable

**Consent for publication:** The manuscript has not been published before and is not being considered for publication elsewhere. All authors have contributed to the creation of this manuscript for important intellectual content and read and approved the final manuscript.

**Availability of data and materials:** The datasets used and/or analysed during the current study are available from the corresponding author on reasonable request.

**Competing interests:** The authors declare that they have no competing interests.

**Funding:** This research was funded by a grant from project 81672154 supported by National Natural Science Foundation of China (NSFC). The authors report no involvement in the research by the sponsor that could have influenced the outcome of this work.

**Authors' contributions:** Shile Cheng and Hao Peng have given substantial contributions to the design of the manuscript. Zhigang Nie and Shile were responsible for writing, figures and literature search. All authors have participated to drafting the manuscript, Shile revised it critically. All authors read and approved the final version of the manuscript.

**Acknowledgements:** Not applicable

## References

1. Moya-Angeler J, Gianakos AL, Villa JC, Ni A, Lane JM. Current concepts on osteonecrosis of the femoral head. *World J Orthop.* 2015;6:590–601.
2. Mankin HJ. Nontraumatic necrosis of bone (osteonecrosis). *N Engl J Med.* 1992;326:1473–9.
3. Chang CC, Greenspan A, Gershwin ME. Osteonecrosis: current perspectives on pathogenesis and treatment. *Semin Arthritis Rheum.* 1993;23:47–69.
4. Fukushima W, et al. Nationwide epidemiologic survey of idiopathic osteonecrosis of the femoral head. *Clin Orthop Relat Res.* 2010;468:2715–24.
5. Chang C, Greenspan A, Gershwin ME. The pathogenesis, diagnosis and clinical manifestations of steroid-induced osteonecrosis. *J Autoimmun.* 2020;110:102460.
6. Shigemura T, et al. Incidence of osteonecrosis associated with corticosteroid therapy among different underlying diseases: prospective MRI study. *Rheumatology.* 2011;50:2023–8.

7. Chen K, et al. Steroid-induced osteonecrosis of the femoral head reveals enhanced reactive oxygen species and hyperactive osteoclasts. *Int J Biol Sci.* 2020;16:1888–900.
8. Zhou Z, et al. IL-15 deficiency alleviates steroid-induced osteonecrosis of the femoral head by impact osteoclasts via RANKL-RANK-OPG system. *Immun Ageing.* 2020;17:19.
9. Tian L, Baek S-H, Jang J, Kim S-Y. Imbalanced bone turnover markers and low bone mineral density in patients with osteonecrosis of the femoral head. *Int Orthop.* 2018;42:1545–9.
10. Wang L, et al. lncRNA PVT1 promotes the migration of gastric cancer by functioning as ceRNA of miR-30a and regulating Snail. *J Cell Physiol.* 2020. doi:10.1002/jcp.29881.
11. Salmena L, Poliseno L, Tay Y, Kats L, Pandolfi P. P. A ceRNA hypothesis: the Rosetta Stone of a hidden RNA language? *Cell.* 2011;146:353–8.
12. Wu X, Sun W, Tan M Noncoding RNAs in Steroid-Induced Osteonecrosis of the Femoral Head. *Biomed Res. Int.* 2019, 8140595 (2019).
13. Xiang S, Li Z, Weng X. The role of lncRNA RP11-154D6 in steroid-induced osteonecrosis of the femoral head through BMSC regulation. *J Cell Biochem.* 2019;120:18435–45.
14. Wang Q, et al. lncRNA expression profiling of BMSCs in osteonecrosis of the femoral head associated with increased adipogenic and decreased osteogenic differentiation. *Sci Rep.* 2018;8:9127.
15. Stelzer G, et al. VarElect: the phenotype-based variation prioritizer of the GeneCards Suite. *BMC Genom.* 2016;17(Suppl 2):444.
16. Youm Y-S, Lee S-Y, Lee S-H. Apoptosis in the osteonecrosis of the femoral head. *Clin Orthop Surg.* 2010;2:250–5.
17. Calder JDF, BATTERY L, Revell PA, Pearse M, Polak JM. Apoptosis—a significant cause of bone cell death in osteonecrosis of the femoral head. *J Bone Joint Surg Br.* 2004;86:1209–13.
18. Weinstein RS, Nicholas RW, Manolagas SC. Apoptosis of osteocytes in glucocorticoid-induced osteonecrosis of the hip. *J Clin Endocrinol Metab.* 2000;85:2907–12.
19. Kawai K, Tamaki A, Hirohata K. Steroid-induced accumulation of lipid in the osteocytes of the rabbit femoral head. A histochemical and electron microscopic study. *J Bone Joint Surg Am.* 1985;67:755–63.
20. McGee-Lawrence ME, et al. Hdac3 deficiency increases marrow adiposity and induces lipid storage and glucocorticoid metabolism in osteochondroprogenitor cells. *J Bone Miner Res.* 2016;31:116–28.
21. Ding L, Morrison SJ. Haematopoietic stem cells and early lymphoid progenitors occupy distinct bone marrow niches. *Nature.* 2013;495:231–5.
22. Abreu-Silva AL, et al. Histopathological studies of visceralized *Leishmania (Leishmania) amazonensis* in mice experimentally infected. *Vet Parasitol.* 2004;121:179–87.
23. Costa AAUM, et al. Experimental model of chronic osteomyelitis caused by *Leishmania (L) amazonensis*. *Acta Trop.* 2006;98:125–9.

24. Okazaki S, et al. Femoral head osteonecrosis can be caused by disruption of the systemic immune response via the toll-like receptor 4 signalling pathway. *Rheumatology*. 2009;48:227–32.
25. Tateda K, et al. The suppression of TRIM21 and the accumulation of IFN- $\alpha$  play crucial roles in the pathogenesis of osteonecrosis of the femoral head. *Lab Invest*. 2012;92:1318–29.
26. Okazaki S, et al. Weight bearing does not contribute to the development of osteonecrosis of the femoral head. *Int J Exp Pathol*. 2012;93:458–62.
27. Okazaki S, et al. Development of non-traumatic osteonecrosis of the femoral head requires toll-like receptor 7 and 9 stimulations and is boosted by repression on nuclear factor kappa B in rats. *Lab Invest*. 2015;95:92–9.
28. Gessner A, Blum H, Röllinghoff M. Differential regulation of IL-9-expression after infection with *Leishmania major* in susceptible and resistant mice. *Immunobiology*. 1993;189:419–35.
29. Geng W, Zhang W, Ma J. IL-9 exhibits elevated expression in osteonecrosis of femoral head patients and promotes cartilage degradation through activation of JAK-STAT signaling in vitro. *Int Immunopharmacol*. 2018;60:228–34.
30. Chen B, Liu Y, Cheng L. IL-21 Enhances the Degradation of Cartilage Through the JAK-STAT Signaling Pathway During Osteonecrosis of Femoral Head Cartilage. *Inflammation*. 2018;41:595–605.
31. Adapala NS, Yamaguchi R, Phipps M, Aruwajoye O, Kim HK. W. Necrotic Bone Stimulates Proinflammatory Responses in Macrophages through the Activation of Toll-Like Receptor 4. *Am J Pathol*. 2016;186:2987–99.
32. Wu X, et al. TNF- $\alpha$  mediated inflammatory macrophage polarization contributes to the pathogenesis of steroid-induced osteonecrosis in mice. *Int J Immunopathol Pharmacol*. 2015;28:351–61.
33. Castaneda OA, Lee S-C, Ho C-T, Huang T-C. Macrophages in oxidative stress and models to evaluate the antioxidant function of dietary natural compounds. *J Food Drug Anal*. 2017;25:111–8.
34. Yang Z, Ming X-F. Functions of arginase isoforms in macrophage inflammatory responses: impact on cardiovascular diseases and metabolic disorders. *Front Immunol*. 2014;5:533.
35. Marathe C, et al. The arginase II gene is an anti-inflammatory target of liver X receptor in macrophages. *J Biol Chem*. 2006;281:32197–206.
36. Halleen JM, et al. Serum tartrate-resistant acid phosphatase 5b is a specific and sensitive marker of bone resorption. *Clin Chem*. 2001;47:597–600.
37. Yin Y, et al. Upregulating MicroRNA-410 or Downregulating Wnt-11 Increases Osteoblasts and Reduces Osteoclasts to Alleviate Osteonecrosis of the Femoral Head. *Nanoscale Res Lett*. 2019;14:383.
38. Fang B, et al. Involvement of tumor necrosis factor alpha in steroid-associated osteonecrosis of the femoral head: friend or foe? *Stem Cell Res Ther*. 2019;10:5.
39. Brijs K, Miclotte I, Vermeire S, Darche V, Politis C. Osteonecrosis of the jaw in patients with inflammatory bowel disease treated with tumour necrosis factor alpha inhibitors. *Int J Oral*

Maxillofac Surg. 2020;49:317–24.

40. Tracey D, Klareskog L, Sasso EH, Salfeld JG, Tak PP. Tumor necrosis factor antagonist mechanisms of action: a comprehensive review. *Pharmacol Ther.* 2008;117:244–79.
41. Boyce BF, et al. TNF-alpha and pathologic bone resorption. *Keio J Med.* 2005;54:127–31.
42. Li W, et al Association of MMP9-1562C/T and MMP13-77A/G Polymorphisms with Non-Small Cell Lung Cancer in Southern Chinese Population. *Biomolecules* **9**, (2019).
43. Du J, et al. Association between genetic polymorphisms of MMP8 and the risk of steroid-induced osteonecrosis of the femoral head in the population of northern China. *Medicine.* 2016;95:e4794.
44. Jiang L, Zhang C, Wei B. Association of MMP-8 rs2012390 and rs11225394 polymorphisms with osteonecrosis of the femoral head risks: Evidence from a meta-analysis. *Medicine.* 2018;97:e12753.
45. An F, et al. MMP8 polymorphism is associated with susceptibility to osteonecrosis of the femoral head in a Chinese Han population. *Oncotarget.* 2017;8:21561–6.
46. Chen J, et al. MMP-3 and MMP-8 single-nucleotide polymorphisms are related to alcohol-induced osteonecrosis of the femoral head in Chinese males. *Oncotarget.* 2017;8:25177–88.
47. Wang K, et al. MMP8 and MMP9 gene polymorphisms were associated with breast cancer risk in a Chinese Han population. *Sci Rep.* 2018;8:13422.

## Tables

Table 1  
Key enrichment pathways and pathways-involved genes by GSEA

Enrichment pathway	Gene symbols of core enrichment
programmed necrotic cell death	PELI1, TICAM2, CD14, MAP3K5, TLR4, LY96, CFLAR, BIRC3, FAS, MLKL, CASP8, PPIF, PYGL, RIPK1, CYLD, ITPK1, TICAM1, FASLG, RBCK1, TLR3, TNF
intracellular lipid transport	ABCG1, PRKAG2, CPT1B, ABCA1, MID1IP1, SGPP1, CES1, ANXA2P2, SERAC1, NPC1, OSBPL2, ANXA2, ABCD3, CPT2, SLC25A20, LDLRAP1, NPC2, NUS1
necrotic cell death	PELI1, TICAM2, CD14, MAP3K5, TLR4, LY96, CFLAR, BIRC3, FAS, MLKL, CASP8, PPIF, PYGL, TMEM123, RIPK1, HEBP2, CYLD, ITPK1, TICAM1, FASLG, RBCK1, TLR3, TNF, TSPO
lymph vessel morphogenesis	FLT4, ACVRL1, PDPN, PPP3CB, EPHA2, FOXC1, PROX1, CCBE1, PROX2, VEGFC, SOX18
hydrogen peroxide catabolic process	EPX, CAT, APOA4, MT3, GPX5, HBM, HBQ1, HBE1, HBZ, MPO, HP, PXDN, SNCA, PRDX2, HBD
lymph vessel development	TBX1, FLT4, EFNB2, ACVRL1, PDPN, PPP3CB, EPHA2, FOXC1, PROX1, CCBE1, PROX2, VEGFC, SOX18
leishmania infection	PTGS2, TLR2, NCF1, HLA-DMB, NCF4, NCF2, TLR4, HLA-DRB3, IFNGR1, JAK2, IFNGR2, FCGR2A, FCGR2C, HLA-DMA, ITGB2, ITGA4, MAPK3, PTPN6, FCGR3A, HLA-DRB5, IL1B, JAK1, TRAF6, PRKCB, FCGR3B, ITGAM, CYBA, HLA-DRA, STAT1, NFKBIA, HLA-DRB1, HLA-DPA1, TGFB1, NFKB1, MYD88, FOS, HLA-DOB, HLA-DQA2, IRAK1, HLA-DRB4, MAPK14, TNF, HLA-DQA1
glycosaminoglycan biosynthesis chondroitin sulfate	CHST7, CHST15, CSGALNACT1, XYLT1, CHSY1, DSE, CHST11, CHST14, B3GALT6, CSGALNACT2
T cell receptor signaling pathway	MAP3K8, PAK1, ICOS, RAF1, LCP2, PIK3R5, CBL, MALT1, MAPK3, PTPN6, BCL10, PAK2, SOS2, CHUK, PIK3CB, NFKBIE, LCK, PTPRC, VAV1, NCK1, LAT, CD28, ITK, NFKBIA, MAP2K1, PIK3CG, GSK3B, PIK3CD, PDPK1, CD3D, NFKB1, NFATC3, CD4, GRB2, CD3G, FOS, FYN,  IKBKB, PPP3CA, CD8B, RASGRP1, PLCG1, MAP3K14, RHOA, AKT1, CD8A, CD247, CD3E, MAPK14, TNF, SOS1, PPP3CC, KRAS, PRKCQ, AKT3, CARD11

Table 2  
Core analysis of DEGs matrix using IPA in SONFH.

<b>Ingenuity canonical pathway</b>	<b>-log (p value)</b>	<b>Ratio</b>	<b>z-score</b>	<b>Molecules</b>
Interferon Signaling	4.12	0.167	2.449	IFIT1, IFIT3, IFNGR1, IFNGR2, MX1, TYK2
Production of Nitric Oxide and Reactive Oxygen Species in Macrophages	3.41	0.0649	3.464	ARG2, IFNGR1, IFNGR2, IRF8, LYZ, NCF1, NCF2, NCF4, RHOQ, SERPINA1, TLR2, TYK2
Fcγ Receptor-mediated Phagocytosis in Macrophages and Monocytes	2.56	0.0753	2.646	FCGR2A, FCGR3A/FCGR3B, HCK, LCP2, LYN, NCF1, PAK1
TREM1 Signaling	2.54	0.0857	2.449	TLR1, TLR2, TLR7, TLR8, TREM1, TYROBP
iNOS Signaling	1.93	0.0909	2	CD14, IFNGR1, IFNGR2, TYK2
Gai Signaling	1.87	0.056	2.646	CXCR2, FPR2, GNG11, HCAR2, P2RY13, RAP1GAP, S1PR3
Neuroinflammation Signaling Pathway	1.81	0.0412	2.333	IFNGR1, IFNGR2, NCF1, NCF2, PTGS2, SNCA, TLR1, TLR2, TLR7, TLR8, TYK2, TYROBP
Tec Kinase Signaling	1.79	0.05	2.449	FCER1A, GNG11, HCK, LYN, PAK1, RHOQ, TNFSF10, TYK2
Dendritic Cell Maturation	1.61	0.0462	2.449	FCGR2A, FCGR2C, FCGR3A/FCGR3B, HLA-DRB3, IGHG3, IRF8, TLR2, TYROBP
Sirtuin Signaling Pathway	1.53	0.0389	-2.333	ARG2, BPGM, DUSP6, FOXO3, GABARAPL2, GADD45A, H1-2, MT-ND1, POLR1D, SLC2A1, STK11

Table 3  
The biology function analysis of IPA.

Categories	Diseases or Functions Annotation	p-value	Predicted Activation State	Activation z-score
Cell-To-Cell Signaling and Interaction	Binding of blood cells	9.03E-11	Increased	2.998
Cell-To-Cell Signaling and Interaction	Adhesion of blood cells	9.37E-11	Increased	2.688
Cell-To-Cell Signaling and Interaction	Binding of myeloid cells	1.57E-09	Increased	2.899
Cellular Movement	Cell movement of blood cells	2.08E-09	Increased	2.111
Cardiovascular System Development and Function, Cell-To-Cell Signaling and Interaction	Activation of vascular endothelial cells	2.99E-05	Increased	2.191
Cardiovascular System Development and Function, Cell-To-Cell Signaling and Interaction	Adhesion of endothelial cells	3.39E-05	Increased	2.124
Cardiovascular System Development and Function, Cell-To-Cell Signaling and Interaction	Binding of vascular endothelial cells	9.35E-05	Increased	2.697
Cell Morphology	Shape change of blood cells	2.49E-03	Increased	2.209
Free Radical Scavenging	Metabolism of reactive oxygen species	7.03E-09	Increased	2.205
Free Radical Scavenging	Production of reactive oxygen species	1.49E-08	Increased	3.007
Free Radical Scavenging	Synthesis of reactive oxygen species	5.24E-08	Increased	2.581
Cardiovascular System Development and Function, Cell-To-Cell Signaling and Interaction	Binding of endothelial cells	6.22E-08	Increased	2.796
Free Radical Scavenging, Molecular Transport	Quantity of reactive oxygen species	6.26E-04	Increased	2.19
Inflammatory Response	Immune response of cells	1.59E-05	Increased	2.07
Cell Death and Survival	Cell death of immune cells	9.15E-05	Increased	2.323

Categories	Diseases or Functions Annotation	p-value	Predicted Activation State	Activation z-score
Inflammatory Response	Inflammatory response	1.64E-04	Increased	2.809
Cardiovascular System Development and Function, Cell-To-Cell Signaling and Interaction	Adhesion of vascular endothelial cells	2.95E-04	Increased	2.078
Cell-mediated Immune Response	T cell development	3.64E-04	Increased	2.135
Cellular Movement	Cell movement of myeloid cells	1.32E-03	Increased	2.375
Cellular Movement	Chemotaxis of myeloid cells	1.44E-03	Increased	2.268

Table 4  
The genes related to SONFH.

Gene symbol	Description	Matched phenotypes	Score	Log10 (p)	Average disease causing likelihood
TNF	Tumor necrosis factor	Femoral head necrosis, necrosis	116.56	4.42	70.40
TNFSF10	TNF superfamily member 10	necrosis	31.34	3.65	52.30
FAS	Fas cell surface death receptor	necrosis	26.35	3.42	44.30
TNFSF13B	TNF superfamily member 13b	necrosis	22.09	3.22	75.30
FASLG	Fas ligand	necrosis	21.95	3.19	63.40
TLR4	Toll like receptor 4	necrosis	19.41	3.08	25.40
CASP8	Caspase 8	necrosis	18.66	3.06	68.60
RIPK1	Receptor interacting serine/threonine kinase 1	necrosis	16.38	2.89	72.70
PTGS2	Prostaglandin endoperoxide synthase 2	necrosis	13.25	2.60	66.50

Table 5  
Gene related to osteonecrosis in MalaCards database.

Gene symbol	Description	Score
BGLAP	Bone gamma-carboxyglutamate protein	14.85
TNFSF11	TNF superfamily member 11	14.75
BMP2	Bone morphogenetic protein 2	14.67
TNFRSF11B	TNF receptor superfamily member 11b	14.60
VEGFA	Vascular endothelial growth factor A	14.34
ACP5	Acid phosphatase 5, tartrate resistant	13.82
COL2A1	Collagen type II alpha 1 chain	13.80
PTH	Parathyroid hormone	13.80
FDPS	Farnesyl diphosphate synthase	13.79
RUNX2	Runx family transcription factor 2	13.73
SERPINE1	Serpin Family E Member 1	13.42
MTHFR	Methylenetetrahydrofolate Reductase	13.15
CYP2C8	Cytochrome P450 Family 2 Subfamily C Member 8	13.09
F2	Coagulation Factor II, Thrombin	13.08
TNF	Tumor Necrosis Factor	13.06
DKK1	Dickkopf WNT Signaling Pathway Inhibitor 1	12.93
ABCB1	ATP Binding Cassette Subfamily B Member 1	12.85
BMP7	Bone Morphogenetic Protein 7	12.74
NOS3	Nitric Oxide Synthase 3	12.65
NFATC1	Nuclear Factor of Activated T Cells 1	12.56
LRP5	LDL Receptor Related Protein 5	12.49
IGF1	Insulin Like Growth Factor 1	12.45
SERPINC1	Serpin Family C Member 1	12.39
CYP3A4	Cytochrome P450 Family 3 Subfamily A Member 4	12.35
FAM201A	Family with Sequence Similarity 201 Member A	12.34
FGF2	Fibroblast Growth Factor 2	12.33
PLG	Plasminogen	12.30

Gene symbol	Description	Score
ENG	Endoglin	12.28
MMP8	Matrix Metalloproteinase 8	12.25
BMP6	Bone Morphogenetic Protein 6	12.14
ESR1	Estrogen Receptor 1	12.14
IL10	Interleukin 10	11.94

Table 6  
Targets of hub genes with experimental evidence were predicated by miRWalk2.0.

Gene symbol	miRNAs
ACP5	/
MMP8	hsa-miR-26b-5p
TNF	hsa-miR-19a-3p
	hsa-miR-452-5p
	hsa-miR-187-3p
	hsa-miR-130a-3p
	hsa-miR-143-3p

Table 7  
Targets of miRNAs were predicated by miRWalk2.0.

Hub genes	Candidate miRNA	Predicated numbers of lncRNAs
ACP5/MMP8/TNF	hsa-miR-7845-5p	None
ACP5/MMP8/TNF	hsa-miR-6772-3p	None
ACP5/MMP8/TNF	hsa-miR-5010-3p	124
ACP5/MMP8/TNF	hsa-miR-4653-5p	None
ACP5/MMP8/TNF	hsa-miR-1587	None
MMP8	hsa-miR-26b-5p	160
TNF	hsa-miR-19a-3p	220
TNF	hsa-miR-452-5p	66
TNF	hsa-miR-187-3p	19
TNF	hsa-miR-130a-3p	117
TNF	hsa-miR-143-3p	250

## Figures

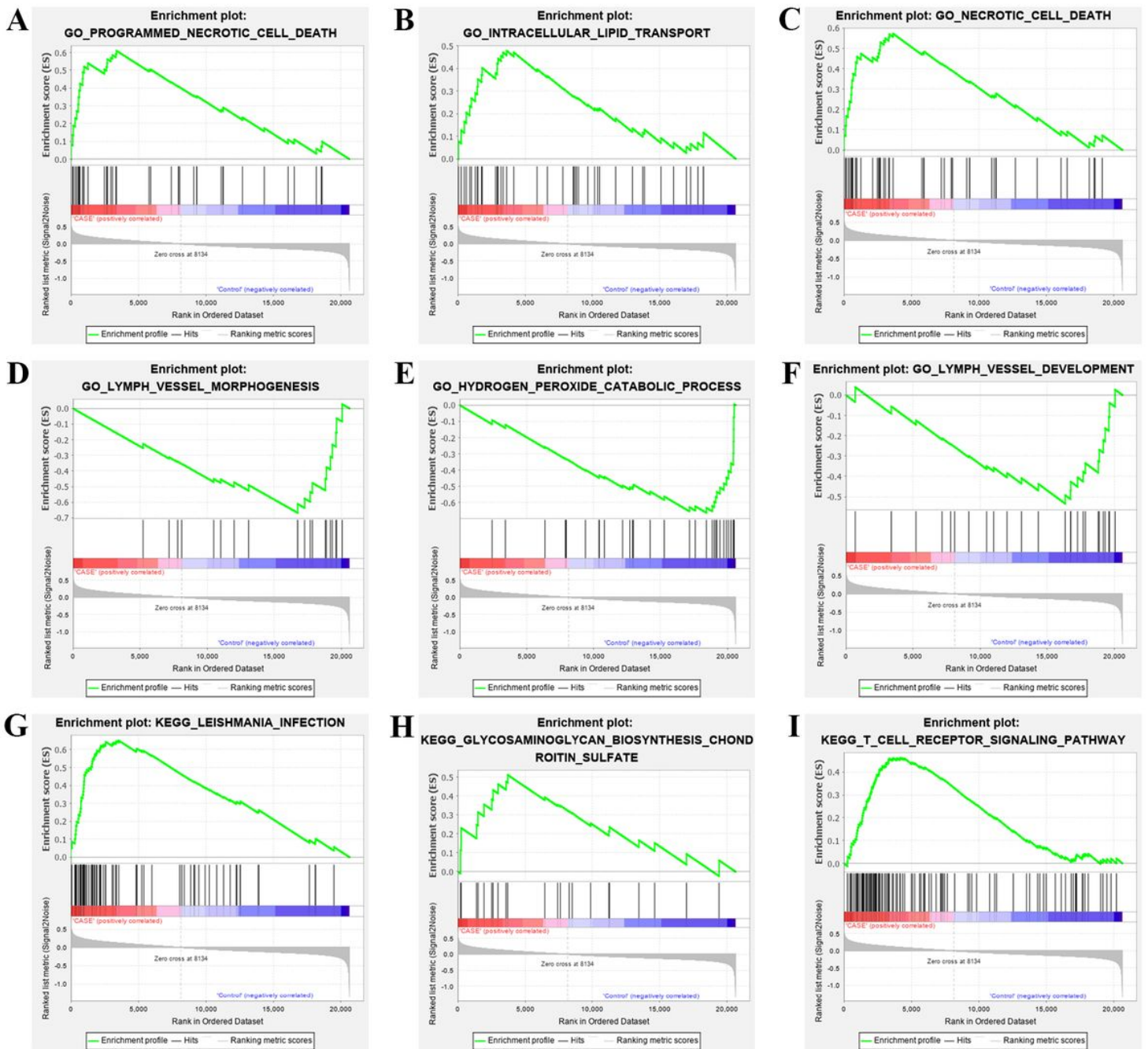


**Figure 1**

DEGs identification and pathway enrichment by GSEA. (A)-(F) The enriched entries were analyzed based on c5.all.v7.1.symbols.gm. (G)-(I) The enriched entries were analyzed based on c2.cp.kegg.v7.1.symbols.gm.

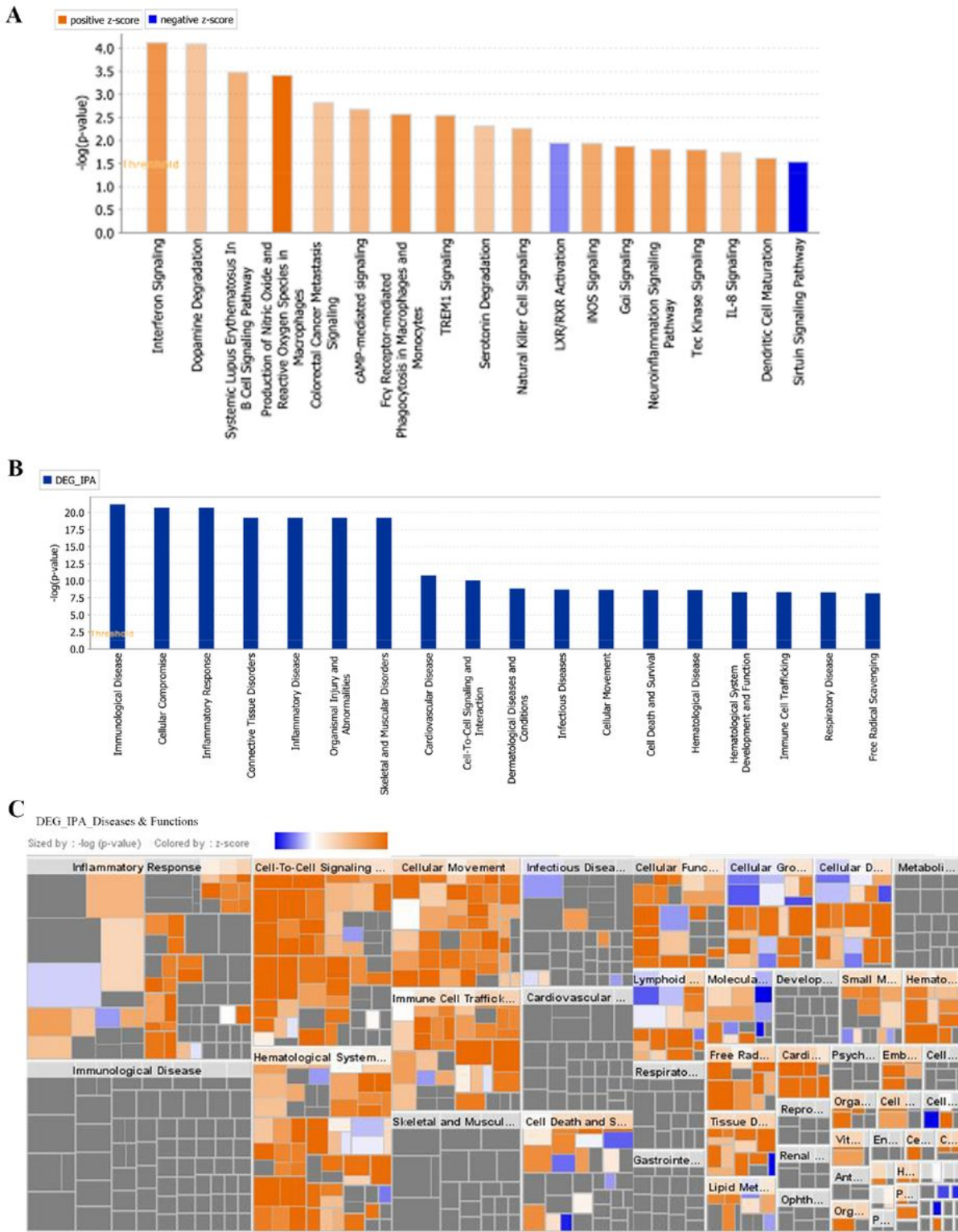


**Figure 2**

Canonical pathway and molecule function analysis by IPA. (A) The canonical pathway analysis and candidate genes screened by IPA. (B) The different expression genes of molecule function were screened by IPA. (C) The modules of molecule function were enriched by IPA.

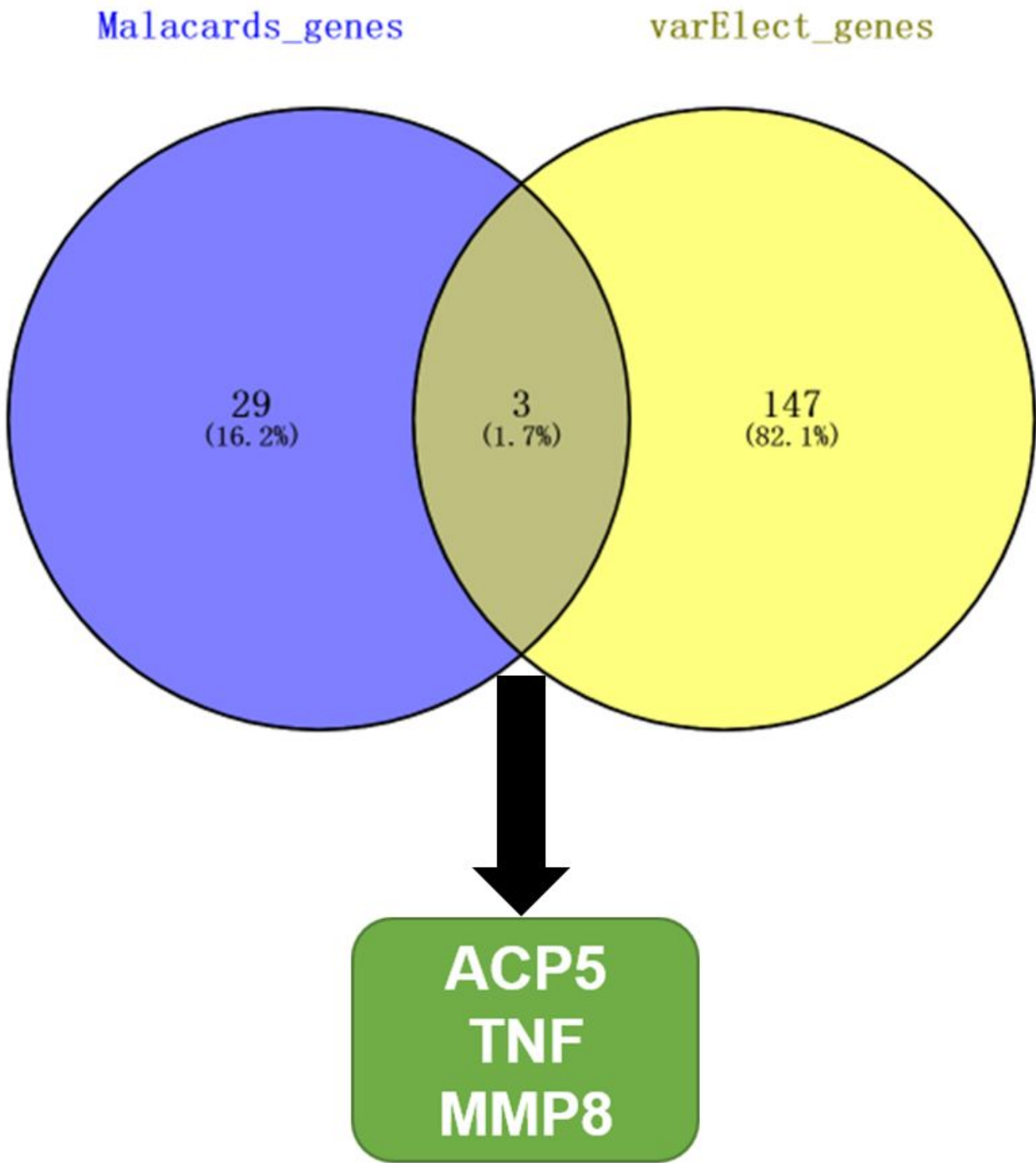


**Figure 3**

Identification of candidate genes of SONFH. The Venn diagrams of two gene sets overlapping.

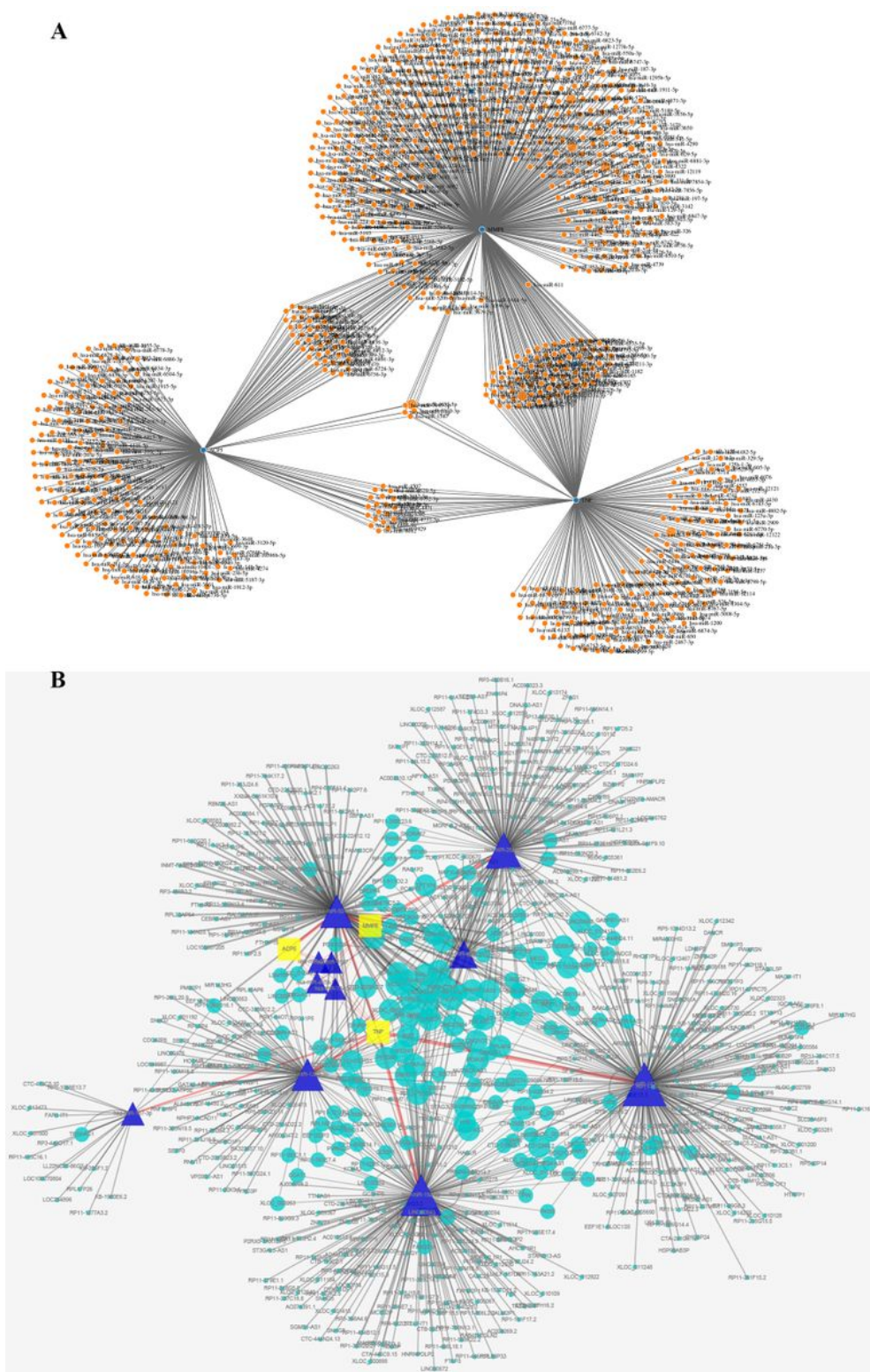


**Figure 4**

Construction of ceRNA network of hub genes. (A) The network between ACP5, TNF, MMP8 and miRNAs. (B) The ceRNA networks among ACP5, TNF, MMP8, miRNAs and lncRNAs.

## Supplementary Files

This is a list of supplementary files associated with this preprint. Click to download.

- [Supplementaryfigure1.pdf](#)